Electronic Supplementary Information

Microfluidic Origami Electrochemiluminescece Aptamer-device Based on Porous Au-Paper Electrode and Phenyleneethynylene Derivative

Jixian Yan, Mei Yan, Lei Ge, Jinghua Yu*, Shenguang Ge, Jiadong Huang

Reagents and apparatus

The aptamer, split into two oligonucleotides, used in this study were purchased from Sangon Biotech Co.,Ltd. (Shanghai, China), and the sequences of the two oligonucleotides were as follows: ss-DNA1, 5'-HS-$(CH_2)_6$-ACCTGGGGGAGTAT-3'; ss-DNA2, 5'-TGCGGAGGAAGGT-NH_2-3'. ATP and cytidine triphosphate (CTP), guanosine triphosphate (GTP), uridine triphosphate (UTP) were purchased from Aladdin Chemistry Co. Ltd.. phenyleneethynylene derivatives (4,4'-(2,5-dimethoxy-1,4-phenylene) bis(ethyne-2,1-diyl)dibenzoic acid; P-acid) modified nanotubular mesoporous Pt-Ag alloy nanoparticles (P-acid/Pt-AgANPs) (P-acid/Pt-Ag ANPs) were prepared according to our previous protocol [1]. Tetrachloroauric acid ($HAuCl_4$) as the precursor for the formation of AuNP seeds and growth solution was purchased from Shanghai Sangon Biological Engineering Technology & Services Co. Potassium ferricyanide, $NaBH_4$, tri-n-propylamine (TPrA), and sodium citrate were products from Shanghai Chemical Reagent Co. Whatman chromatography paper #1 was purchased from GE Healthcare Worldwide and used with further adjustment of size (A4 size).

Disign and Fabrication of μ-OECLD

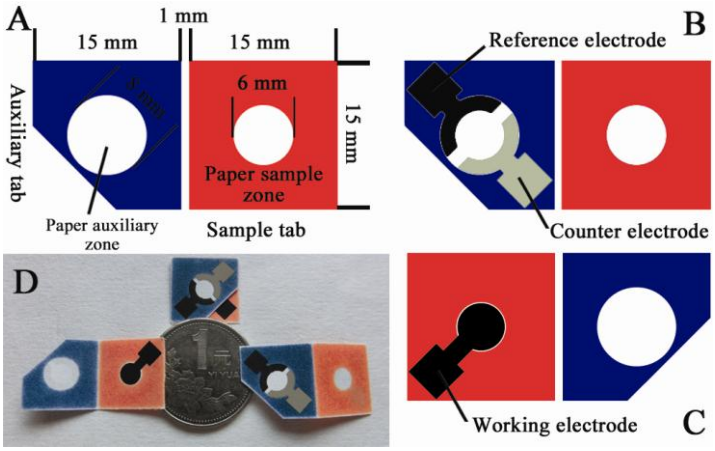

Scheme S1. (A) The schematic representation, size and shape of this μ-OECLD. (B) One side of the μ-OECLD with the screen-printed reference and counter electrode; (C) The reverse side of (B) with the screen-printed working electrode; (D) Pictures of this μ-OECLD.

The preparation of this μ-OECLD was similarly to our previous work [2] with modifications and a detailed procedure was described below. Wax was used as the paper hydrophobization and insulation agent in this work to construct hydrophobic barrier on paper. As shown in Scheme S1A, this origami device was comprised of a square auxiliary tab (15.0 mm × 15.0 mm) and a square sample tab (15.0 mm × 15.0 mm). An angle of the square auxiliary tab was cut off for exposure of the contact pad of screen-printed carbon working electrode (Scheme S1D). The shape of hydrophobic barrier on origami device, which contains a paper auxiliary zone (8 mm in diameter) on auxiliary tab, a paper sample zone (6.0 mm in diameter) on the sample tab, respectively, was designed using Adobe illustrator CS4. The entire origami device could be produced in bulk on an A4 paper sheet by a commercially available solid-wax printer (Xerox Phaser 8560N color printer) (Figure S1). Owing to the porous structure of paper, the melted wax can penetrate into the paper network to decrease the hydrophilicity of paper remarkably (Figure S2) [3]. After the curing process, the unprinted area (paper auxiliary zone and paper sample zone) still maintained good

hydrophilicity, flexibility, and porous structure and will not affect the further screen-printing of electrodes and modifications [3].

Between the sample tab and auxiliary tab, the unprinted line (1 mm in width) was defined as fold line, which could ensure that the paper sample zone on the sample tab was properly and exactly aligned to the auxiliary zone on auxiliary tab after folding (Scheme S1A), due to the difference of flexibility between the printed and unprinted area after baking. The unprinted hydrophilic area (paper auxiliary zone and paper sample zones) constituted the reservoir of the paper electrochemical cell (~40 μL) after being folded at the predefined fold line. Then, the wax-penetrated paper sheet was ready for screen-printing of electrode containing the wire and contact pad on its corresponding paper zone (Scheme S1B,C). Due to the small size of the origami device, the silver wire and contact pad in traditional screen-printed electrode [4] were unnecessary and can be directly replaced by carbon ink and Ag/AgCl ink respectively [5]. The electrode array consisted of a screen-printed Ag/AgCl reference electrode and carbon counter electrode on the auxiliary zone (Scheme S1B and Figure S3) and screen-printed carbon working electrode (5 mm in diameter) on the reverse side of paper sample zone (Scheme S1C and Figure S4), respectively. After folding, the three screen-printed electrodes (working electrode, reference electrode, and counter electrode) will be connected once the paper electrochemical cell was filled with solution. Finally, the paper sheet was cut into individual origami device for further modifications (Scheme S1D).

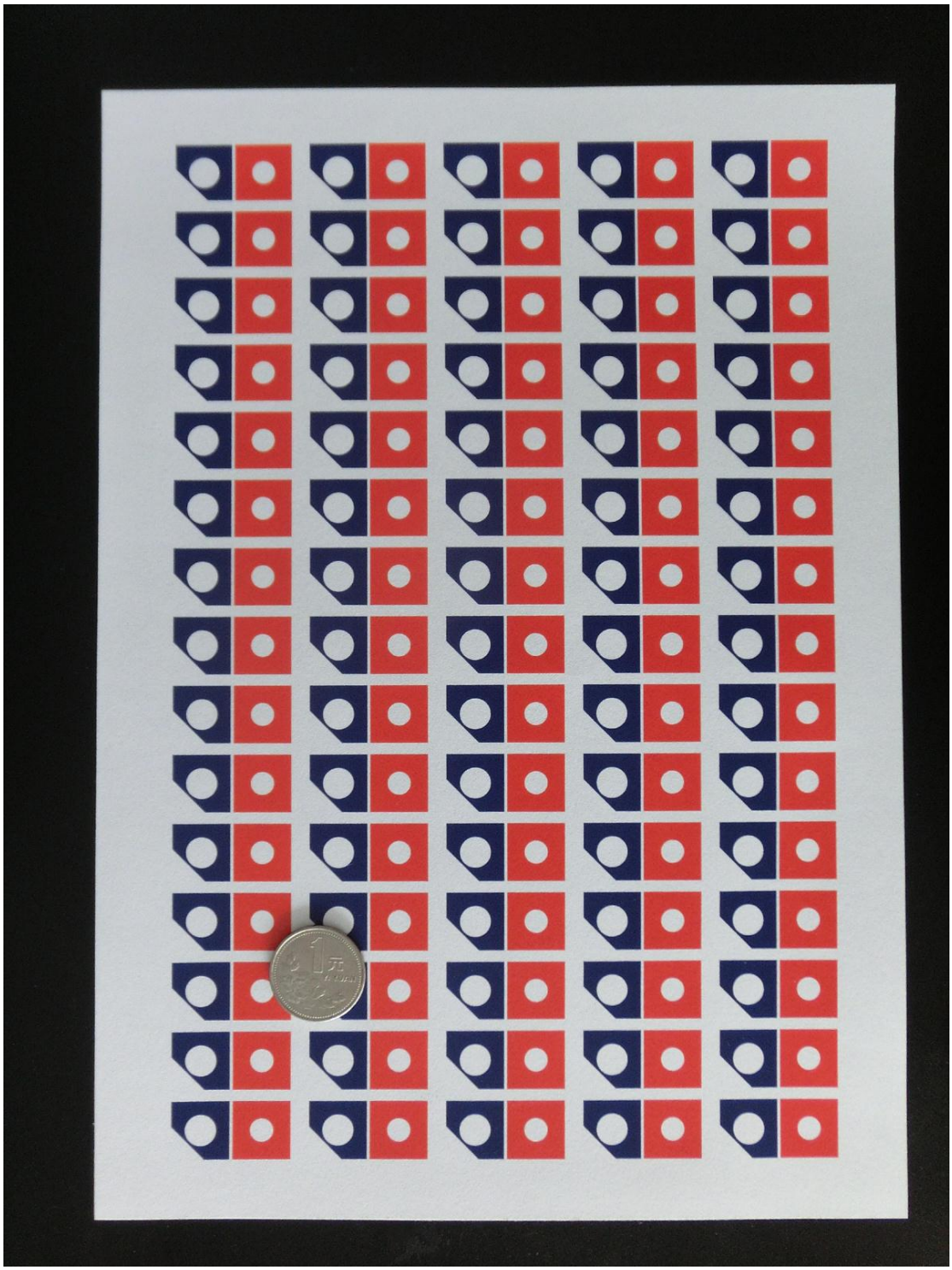

Figure S1. Wax-printed μ-OECLDs on a paper sheet (A4) before baking.

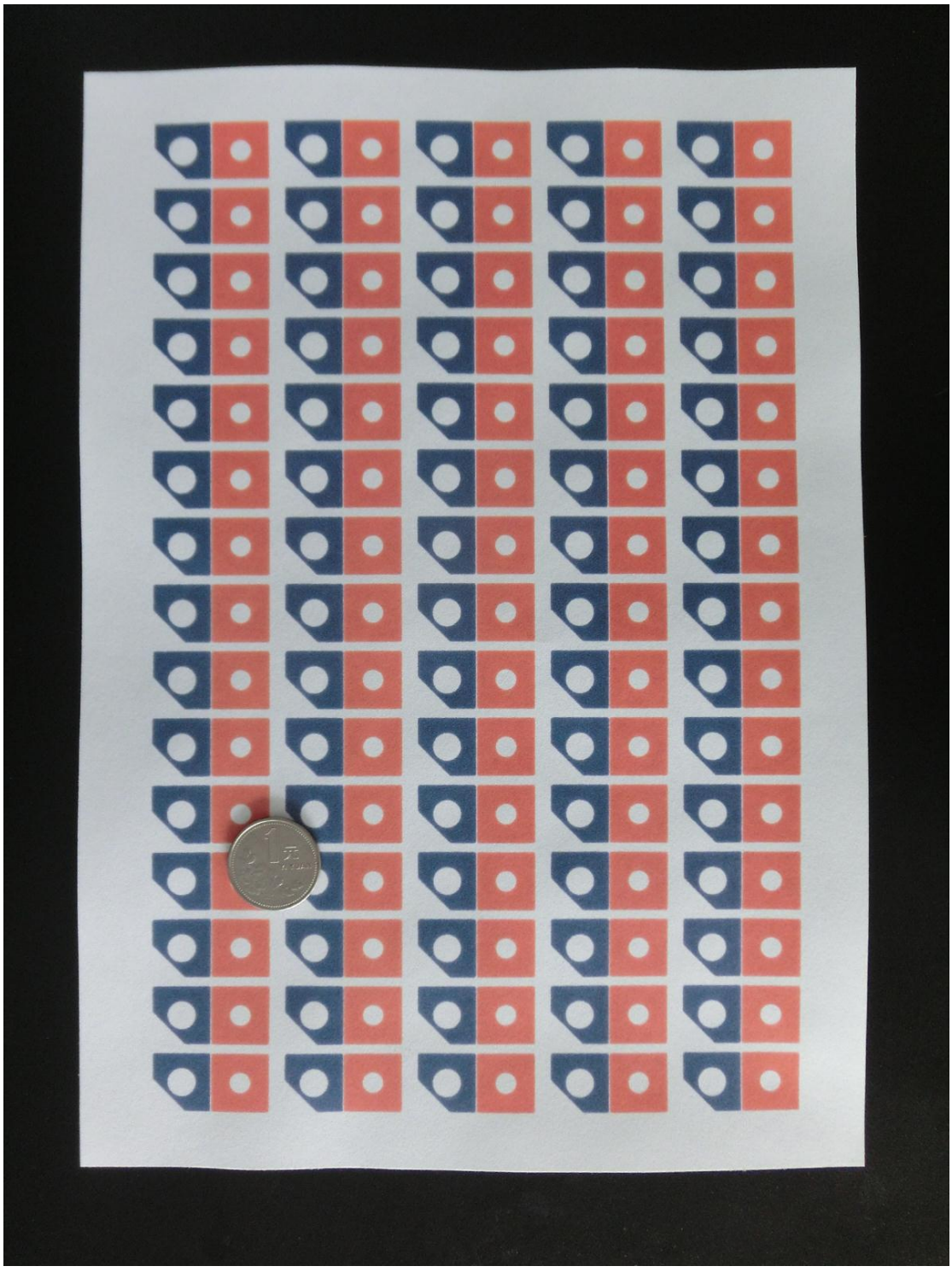

Figure S2. Wax-printed μ-OECLDs on a paper sheet (A4) after baking.

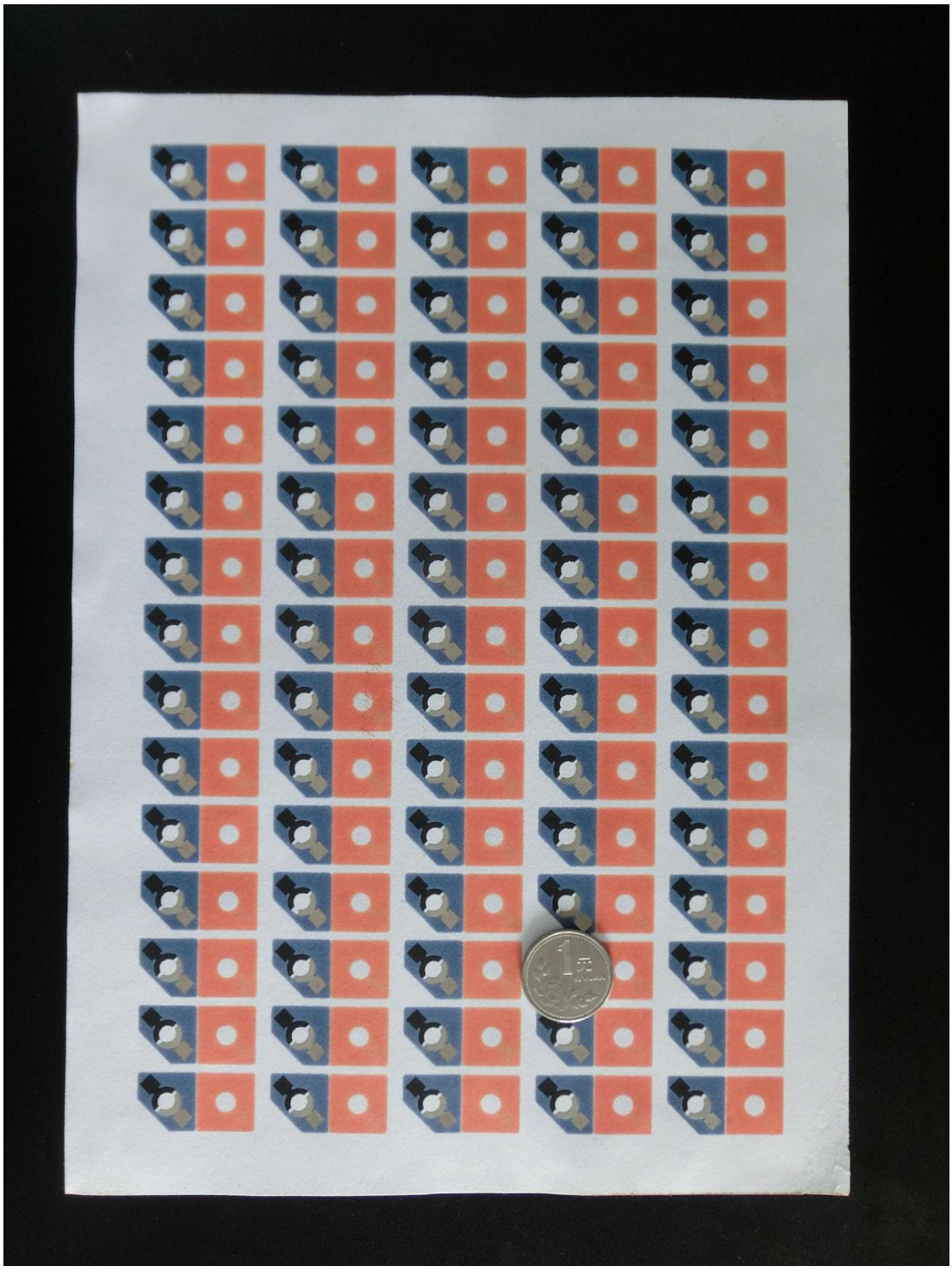

Figure S3. μ-OECLDs on a paper sheet (A4) after screen-printing of Ag/AgCl auxiliary electrodes and carbon counter electrodes on one surface of paper.

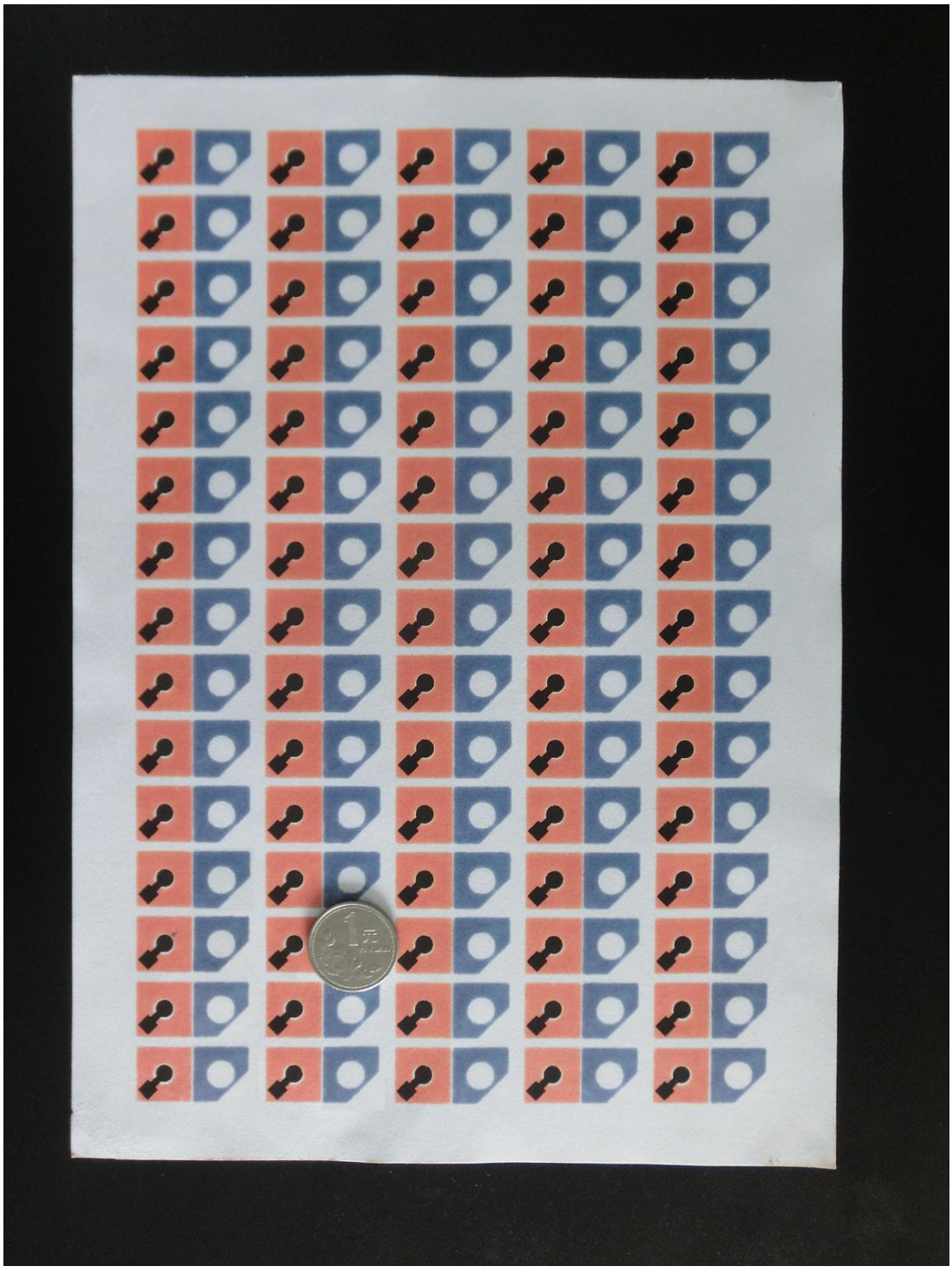

Figure S4. μ-OECLDs on a paper sheet (A4) after screen-printing of carbon working electrodes on the reverse side of paper.

Fabrication of the porous Au-PWE on μ-OECLD

As shown in Scheme 1, the porous Au-PWE was fabricated through growth of an Au NPs layer on the surfaces of cellulose fibers in the paper sample zone of PWE to enhance the conductivity and enlarge the effective surface area of bare PWE. The fabrication procedures of the porous Au-PWE were described as follows: First, The suspension of Au NP seeds was prepared by using $NaBH_4$ as reductant and stabilized with sodium citrate according to the literature [6]. Then, 15.0 μL as-prepared Au NP seeds solution were dropped into the paper sample zone of bare PWE (Scheme 1A), respectively. Then the origami device was equilibrated at room temperature for 1 h to optimize the surface immobilization of Au NP seeds on cellulose fibers. After rinsing with water thoroughly according to the method in our previous work [7] to remove loosely bound Au NP seeds, 15 μL freshly prepared growth aqueous solution of 10 mM PBS (pH 7.0) containing 1.2 mM $HAuCl_4$, 2.0 mM cetyltrimethylammonium chloride and 7.2 mM H_2O_2 for seeds growth were applied into the Au NP seeded PWE, and incubated at room temperature for 10 min. Subsequently, the resulting porous Au-PWE was washed with water thoroughly. Thus a layer of interconnected Au NPs on cellulose fibers with good conductivity were obtained (Scheme 1B), which were dried at room temperature for 20 min.

The scanning electron microscopy (SEM) images of this μ-OECLD were recorded on a JEOL JSM-5510 scanning electron microscope. Transmission electron microscopy (TEM) investigations were performed using JEOL 4000 EX microscope. Electrochemical impedance spectroscopy (EIS) was performed on an IM6x electrochemical working station (Zahner Co., Germany). To measure the resistivity of Au modified paper sample zone, Au modified rectangular wax-penetrated paper zones (1.0 mm×20.0 mm) with screen-printed carbon ink on one side were fabricated through the

growth of an interconnected Au layer on the surfaces of cellulose fibers in these rectangular paper zones under the same conditions in each case, the average resistivity of which equaled to the resistivity of Au modified paper sample zone of Au-PWE in this work. The measurement was performed using a DT-830 multimeter (UniVolt, Japan).

Characterizations of the Au-PWE

The TEM image of Au NP seeds (Figure S5A) revealed a highly mono-dispersed AuNPs suspension with an average diameter of ~3.5 nm. As shown in Figure S5B, the porous bare paper in paper sample zone, possessed high surface area with rough cellulose fibers, could offer an excellent adsorption microenvironment for the Au NP seeds. It can be seen that there was no apparent structural and surface difference between the bare (Figure S5B) and the AuNPs seeded cellulose fibers (Figure S5C) due to the small particle size of Au NP seeds (Figure S5D). In addition, the successful immobilization of Au NP seeds on cellulose fibers was verified by X-ray photoelectron spectroscopy (XPS) and the peaks observed at 82.5 and 86.3 eV are ascribed to metallic gold (Figure S6).

The growth process of the Au NPs layer on the surface of Au NPs seeded cellulose fibers was tracked by scanning electron microscopy (SEM) (Figure S7). As the growth time increased (from 0 to 5 min), the Au NP seeds were rapidly enlarged by incubating in the growth solution under the self-catalytic reduction mechanism of Au NPs growth (Figure S7A,B). Finally, a continuous and dense conducting AuNPs layer with interconnected Au NPs was obtained completely on the cellulose fiber surfaces after 10 min of growth (Figure S7C,D). Figure S8 depicted the CV of the Au-PWE acquired at scan rate 50 $mV \cdot s^{-1}$ in 50 mM phosphate buffer solution (pH 9.2). As shown

in Figure S8, the two peaks at 0.88 and 0.27 V resulting from the oxidation and reduction of the Au ascertained electrochemically the presence of Au in PWE [8].

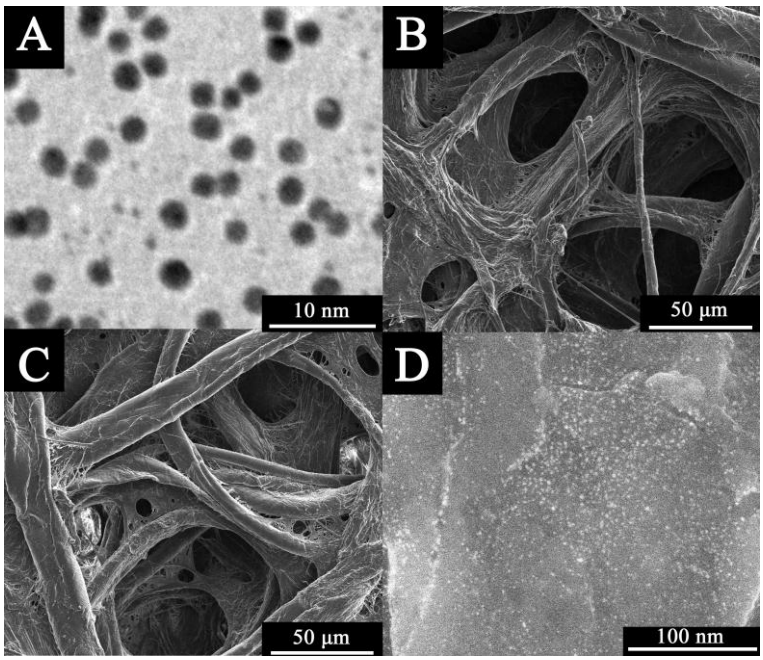

Figure S5. (A) The TEM image of AuNP seeds. The SEM image of (B) bare PWE, (C) AuNP seeded PWE, and (D) AuNP seeds on the surface of the cellulose fiber.

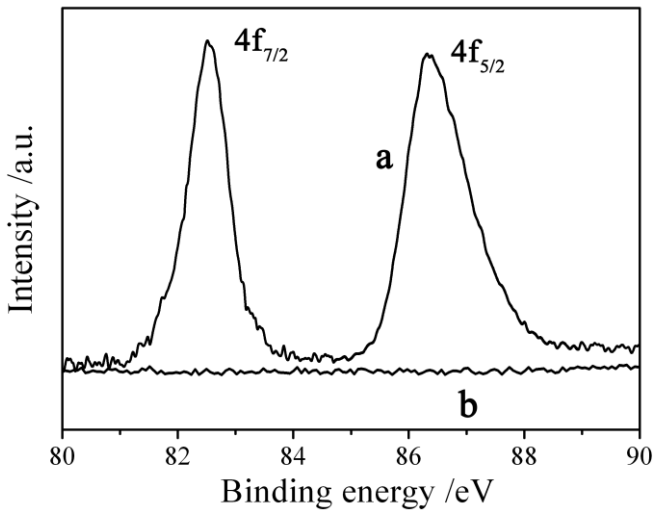

Figure S6. (A) XPS of the (a) Au NP seeded PWE and (b) bare PWE;

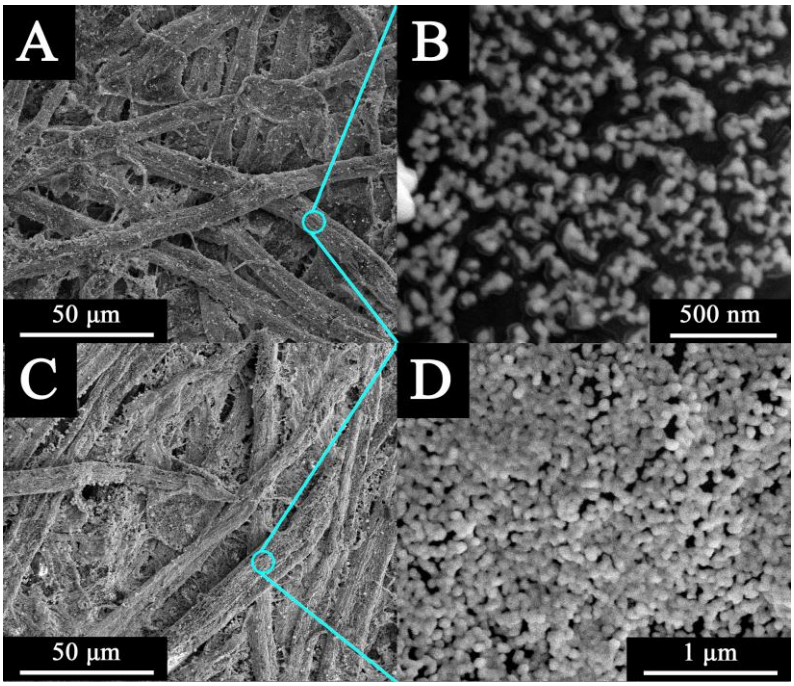

Figure S7. Enlarged Au NPs on the surfaces of the cellulose fibers in PWE at different growth time under different magnification: (A, B) After 5 min of growth; (C, D) After 10 min of growth.

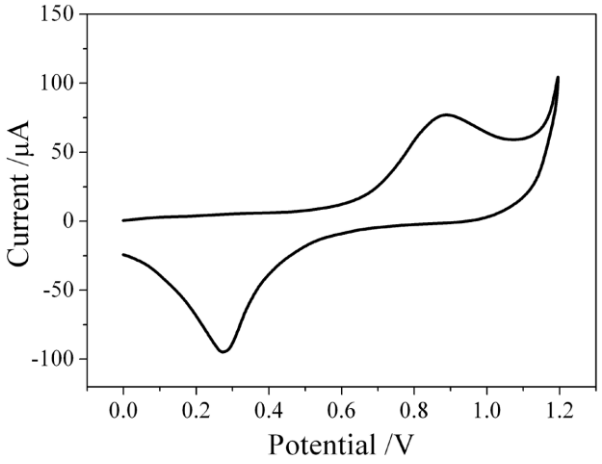

Figure S8 CV of Au-PWE toward 50.0 mM phosphate buffer solution (pH 9.2). Scan rate: 50 $mV \cdot s^{-1}$.

Preparation of P-acid/Pt-Ag ANP labels

The P-acid/Pt-Ag ANP labels were prepared according to our previous work [1]. The N,N'-carbonyldiimidazole activated P-acid/Pt-AgANPs were immediately redispersed into ssDNA2 (3 mL, 50 μM) solution and then incubated for 2 h to form the ssDNA2/P-acid/Pt-AgANPs. The resulting ssDNA2/P-acid/Pt-AgANPs were washed with 10 mM PBS (pH 7.4) and then redispersed in 10 mM PBS (pH 7.4, 1 mL) and stored at 4 ° C before use.

Preparation of microfluidic origami ECL aptamer-device (μ-OECLAD)

The μ-OECLAD was constructed by immobilizing the ssDNA1 into the paper sample zone of porous Au-PWE (Scheme 2C). First, 15 μL of 2 μM ssDNA1 solution was dropped into the porous Au-PWE and kept it for 1 h to form an Au-thiol monolayer. Subsequently, physically absorbed excess ssDNA1s were rinsed with PBS. Then, the resulting μ-OECLAD was stored at 4 ◦C prior to use.

EIS of the μ-OECLAD

EIS of the resulting μ-OECLAD could give detail information about the modification process. EIS were carried out in a background solution of 5 mM $[Fe(CN)_6]^{3+/4+}$ at a bias potential of 170 mV (versus Ag/AgCl). The frequency range was 100 MHz to 10 KHz. In EIS, the diameter of the semicircle at higher frequencies corresponds to the electron-transfer resistance (R_{et}); a change in the value of R_{et} is associated with the blocking behavior of the modification processes in the PWE, and is reflected in the EIS as a change in the diameter of the semicircle at high frequencies.

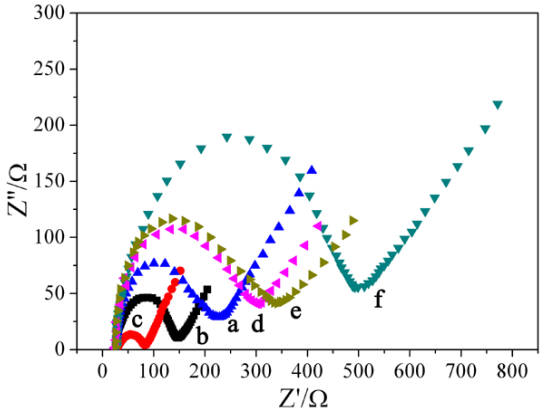

Figure S9. EIS of the PWE under different condition in 10.0 mM $[Fe(CN)_6]^{3+/4+}$ solution containing 0.5 M KCl: (a) bare PWE, (b) Au-PWE after 5 min of grouth, (c) Au-PWE after 10 min of grouth, (d) ssDNA1 modified Au-PWE, (e) ssDNA1 modified Au-PWE after the addition of ssDNA2 in absence of ATP, (f) ssDNA1 modified Au-PWE after the addition of ssDNA2 in presence of ATP.

Herein, the electron-transfer of $[Fe(CN)_6]^{3+/4+}$ onto the surfaces of porous Au-PWE was blocked by the formation of ssDNA1/ATP/ssDNA2 sandwich composites, which resulted in an increase in R_{et}. Figure S9 shows the EIS (presented in the form of the Nyquist plot) of different surface condition of the cellulose fibers in the PWE. The EIS of bare PWE revealed a relatively small semicircle domain (curve a). After the growth of an Au NPs layer, the EIS exhibited an obvious decrease in R_{et} (curve b and curve c). These results were accordant with CV assays as described in the main text. Remarkable increase in the R_{et} value was observed after the immobilization of thiol-modified ssDNA1 (curve d) on the surfaces of Au NPs coated cellulose fibers in porous Au-PWE, indicating that the negatively charged phosphate backbone of the oligonudeotides increased the electron-transfer distance. After being incubated with the solution of ssDNA2 in the absence of ATP, only little amount of ssDNA2 were captured in the PWE through physical adsorption with ssDNA1, thus the electron-transfer kinetics of the redox probe was slow down slightly (curve e). The obvious increase of R_{et} from curve d to curve f could be attributed to the formation of stable and nearly insulating ssDNA1/ATP/ssDNA2 sandwich composites layer

through the ATP-induced split aptamer chips combination on the surfaces of Au-coated cellulose fibers.

ECL assay procedures of this μ-OECLAD

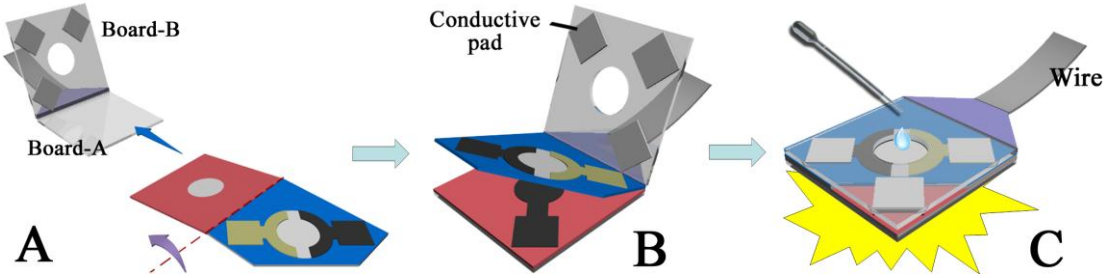

Scheme S2. Schematic representation of the assay procedures for this μ-OECLAD: (A) The sample tab was folded down below the auxiliary tab; (B) The μ-OECLAD was clamped into the device holder; (C) TPrA was added into the paper electrochemical cell to trigger the ECL reaction.

The ECL assay procedures on μ-OECLAD were shown in Scheme 1 and Scheme S2, and a detailed procedure was described as below: First, sample solutions (5 μL) contained different concentrations of ATP was mixed with ssDNA2/P-acid/Pt-AgANPs solution (10 μL). Then the mix solution was added into the modified paper sample zone in PWE and allowed to incubate for 140 s followed by washing thoroughly with PBS for preventing the nonspecific binding and achieving the best possible signal-to-background ratio. Thereafter, the sample tab was folded down below the auxiliary tab and clamped into a home-made device-holder (Scheme S2), which was comprised of two circuit boards (named Board-A and Board-B respectively below) with conductive pads on Board-B, to fix and connect this origami device to the electrochemical workstation (Shanghai CH Instruments Co., China). A PBS solution (40 μL) containing 0.01 mM TPrA was dropped into the paper electrochemical cell through the hole in Board-B (Scheme S2C) and then the device-holder was placed in front of the photomultiplier tube (PMT; detection range: 300–650 nm) that was biased at 800 V. The ECL reaction in the PWE was triggered in the

scanning range 0 - 1.0 V using an MPI-E multifunctional electrochemical and chemiluminescent analytical system (Xi'an Remex Analytical Instrument Ltd. Co.).

Specificity, reproducibility, and stability of this μ-OECLAD

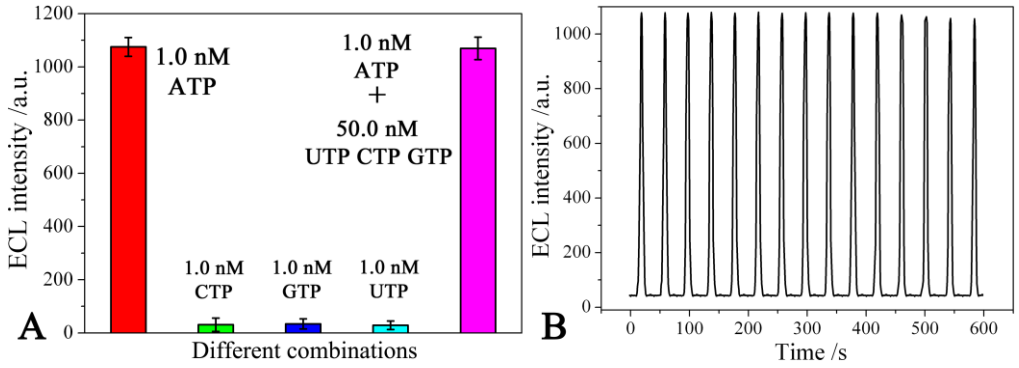

Figure S10. (A) The selectivity of μ-OECLAD to ATP. (B) ECL versus time curve of this μ-OECLAD at an ATP concentration of 1.0 nM over repeated CV scans.

In order to verify the specificity of the μ-OECLAD modified with aptamer for ATP, experiments were performed by using three other ATP analogues in human serum: cytidine triphosphate (CTP), guanosine triphosphate (GTP), and uridine triphosphate (UTP). Figure S10A compared the ECL responses of the μ-OECLAD after incubation with CTP, GTP, and UTP solutions under the same experimental conditions and at the same concentration of 1.0 nM. Figure S10A showed that CTP, GTP, and UTP did not exhibit any great increase of ECL intensity. In contrast to the incubation of this μ-OECLAD with 1 nM ATP, the ECL intensity greatly increased. Similarly, a mixed sample (1.0 nM ATP coexisted with 50.0 nM CTP, GTP, and UTP) did not exhibit major signal change compared with that of ATP alone. This comparison essentially suggested that this μ-OECLAD was highly selective and had quite an affinity toward ATP.

The reproducibility of this μ-OECLAD for ATP was investigated with inter-assay precision. The RSD for the parallel detections of 0 M, 5.0×10^{-11} M, and 1.0×10^{-9} M ATP with ten μ-OECLADs was 3.12%, 2.75%, and 2.91%, respectively. After the μ-OECLAD was continuous

scanned for 15 cycles (Figure S10B), stable and high ECL signals were observed, demonstrating that this μ-OECLAD possessed good stability and was suitable for ECL detection. When this μ-OECLAD was stored and measured at intervals of three days, no obvious change was observed after 4 weeks under ambient conditions. These results indicated that this μ-OECLAD has better reproducibility, stability, and precision during manufacture, storage or long-distance transport to remote regions and developing countries.

Reference

1 M. Yan, L. Ge, W. Gao, J. Yu, X. Song, S. Ge, Z. Jia and C. Chu *Adv. Funct. Mater.*, 2012, **22**, 3899-3906.
2 J. Lu, S. Ge, L. Ge, M. Yan and J. Yu *Electrochimica Acta*, 2012, 80, 334-341.
3 E. Carrilho, A. W. Martinez and G. M. Whitesides *Anal. Chem.*, 2009, **81**, 7091-7095.
4 Z. Nie, F. Deiss, X. Liu, O. Akbulut and G. M. Whitesides *Lab Chip*, 2010, **10**, 3163-3169.
5 L. Ge, J. Yan, X. Song, M. Yan, S. Ge and J. Yu *Biomaterials*, 2012, **33**, 1024-1031.
6 B. D. Busbee, S. O. Obare and C. J. Murphy *Adv. Mater.*, 2003, **15**, 414-416.
7 J. Yan, L. Ge, X. Song, M. Yan, S. Ge and J. Yu *Chem. Eur. J.*, 2012, **18**, 4938-4945.
8 X. Sun, Y. Du, S. Dong and E. Wang *Anal. Chem.*, 2005, **77**, 8166-8169.